Topical Conference on Electronuclear
Physics with Internal Targets,
SLAC, January 1989

CONF-8901115--7

RESULTS FROM FNAL E745 ON NEUTRINO-NUCLEUS INTERACTIONS (EMC EFFECT AND HADRON FORMATION)

CONF-8901115--7

DE90 003836

T.Kitagaki,
Bubble Chamber Physics Laboratory, Tohoku University, Sendai, 980 Japan

(FNAL E745 collaboration)

S.Nakai[9], T.Akagi[9], P.Allen[1], E.D.AlyeaJr.[3], M.Aryal[1], J.E.Brau[8], D.Brick[1], W.M.Bugg[8], A.Chen[1], H.O.Cohn[7], G.T.Condo[8], K.De[1], A.DeSilva[1], Y.C.Du[8], S.Fukui[6], K.Furuno[9], N.Gelfand[2], D.Goloskie[5],E.S.Hafen[5], H.Hanada[9], T.Handler[8], H.J.Hargis[8], E.L.Hart[8], J.Harton[5], K.Hasegawa[9], M.Higuchi[10], Y.Hoshi[10], J.Katayama[9], H.Kawamoto[9], R.Kroeger[8], R.Majoras[8], S.W.Mao[4], Y.Morita[9], L.G.Mu[4], T.Murphy[2], T.Nakajima[9], I.A.Pless[5], M.Sasaki[9], M.Sato[10], A.Shapiro[1], J.Shimony[8], H.Suzuki[9], Y.S.Tai[4], T.Takayama[9], K.Tamae[9], K.Tamai[9], S.Tanaka[9] S.Wang[4], M.Widgoff[1], Y.Wu[4], S.W.Xu[4], A.Yamaguchi[9], M.Zhao[4]

1 Brown University, Providence, RI 02912, USA
2 Fermilab, Batavia, IL 60510, USA
3 Indiana University, Bloomington, Indiana 47405, USA
4 Institute for High Energy Physics (IHEP), Beijing, PRC
5 Massachusetts Institute of Technology, Cambridge, MA 02139, USA
6 Sugiyama Jogakuen University, Nissin, Aichi 470-01, Japan
7 Oak Ridge National Laboratory, Oak Ridge, TN 37831, USA
8 University of Tennessee, Knoxville, TN 37996-1200, USA
9 Tohoku University, Sendai 980, Japan
10 Tohoku Gakuin University, Tagajyo 985, Japan

ABSTRACT

The dark tracks (stubs) in high energy neutrino-nucleus interactions in the Tohoku High Resolution Freon Bubble Chamber are investigated. Classifying events into groups by using the dark tracks, correlations between the dark track production and neutrino interactions are studied. Events without dark tracks comprise a reasonable sample of events which occurred on quasi-free nucleons inside nucleus. By comparing the groups using the no dark track group as a comparison sample instead of neutrino-deuterium events, the EMC effect and hadron formation are investigated. This method provides new results which differ somewhat from the conventional data for the EMC effect and formation-rescattering.

AC02-76CH03000
AS05-76ER03956
AC05-84OR21400

INTRODUCTION

High energy neutrino-nucleus interactions have a unique advantage in the investigation of intranuclear phenomena when compared with hadron or photon interactions and even with charged lepton interactions. This is because the nucleus is quite transparent before the sudden interaction on a quark, and because the interactions are selective for quark flavor. The neutrino-nucleon interaction tells the kinematical detail of primary interaction, the four momentum transfer, Q^2, energy transfer ν, and the direction of current. This experiment, FNAL E745, is a high energy neutrino experiment employing a Freon bubble chamber. The bubble chamber has the unique advantage of 4π detection as well as efficient detection of very short nuclear deexcitation tracks. The observation of dark tracks (nuclear debris) gives us semi-inclusive information on the type of nucleon involved in the interaction. In a previous paper[1], we discussed the EMC effect in neutrino-nucleus interactions. There, the dark tracks at the interaction vertex were used as an indicator of the (volume) interactions which occurred on strongly bound nucleons in the nucleus, while the events without dark track were considered to be (surface) interactions with quasi-free nucleons. This was a new method to investigate the EMC effect, and provided data which differed from conventional experiments. In this paper, we will study the further details on the dark track production and their correlation with neutrino interactions. In these data, we will review the EMC effect again. Also, the formation and rescattering of hadrons inside nucleus will be investigated using the same method. The hadronization/formation of particles from quarks is one of the old but most fundamental problems in particle physics. There have been extensive experimental studies on hadronization[2], however, there has yet to be a definitive experiment. In this paper, we present direct results on hadronization in neutrino-nucleus interactions. Our method is the comparson of two groups of events obtained from a single experiment, therefore providing bias-free results.

EXPERIMENTAL PROCEEDURE

In FNAL experiment E745, the Tohoku 1.4m High Resolution Freon Bubble Chamber Hybrid System was exposed to the wide band neutrino beam generated by 800GeV protons from the TEVATRON. The bubble chamber employed a holographic high resolution camera in addition to three normal stereo-optic cameras, Fig.1. The neutrino beam arrived in three beam pulses of 2ms width with 10sec interval per acceleration cycle of 57sec. The holographic pictures were take- only upon receipt of an interaction trigger. This trigger was produced by a scintillation counter system when charged particles left the chamber without any being incident on it. The holograms, using a 10J Ruby laser, were taken approximately 200μs after the occurrence of an interaction, when the bubble size was still of the order of 50μm. On the other hand normal pictures were taken at the end of every beam pulses when the bubble size had grown to 300μm. About 40% in neutrino events gave rise to good usable holograms.

Kinematical analysis

The analysis of events proceeded in the canonical way for bubble chamber neutrino events. In order to obtain the purest possible sample of neutrino events, our data are restricted to charged current events in this report. Neutrino charged current events were selected by a kinematical method[3]. First, the muon was kinematically defined unless it was identified by the downstream muon detector. This requires that the muon has the largest transverse momentum against the hadron

system in a charged current event. The purity of the selected muon sample is 97% according to a Monte Carlo simulation. After defining a muon, the neutrino energy, E_ν, was calculated from the momentum balance of the visible tracks,

$$E_\nu = P_L^{\mu} + P_L^{vis} + (P_T^{miss}) \cdot P_L^{vis}/P_T^{vis},$$

where P_L and P_T are the longitudinal and transverse momenta relative to the neutrino direction, and the suffices, μ, vis and miss, indicate muon, visible hadrons and missing particles, respectively.

Other kinematical quantities, the four momentum transfer Q^2, energy transfer ν, hadron system mass W, Bjorken x ($x=Q^2/2M\nu$), etc. were deduced from the E_ν. Finally, severe cuts, $W^2>4$ GeV^2 and $P_{TR}>2.5$GeV/c, were applied to events to ensure the rejection of neutral current events and hadron events. This method uses visible hadron tracks, however E_ν is essentially derived from muon momentum and the results of this analysis are equivalent to those of charged lepton scattering experiments. In this experiment (FNAL E745), $<E_\nu>=128$GeV, $<Q^2>=27$(GeV/c)^2, $<\nu>=54$GeV, $<W>=7.7$GeV, $<P_W>=54$GeV/c and $<\gamma_W>=6.0$,

where P_W and γ_W are the momentum and Lorentz factor of the hadron system. The current region moves faster than these and the target region moves slower. Fig.3 shows the distributions of E_ν, Q^2, ν, W and γ_W in this experiment, and Fig.4 shows their interrelationship.

DARK TRACKS

In this experiment the Freon liquid was a mixture of R116, C_2F_6 (27% by weight) and R115, $C_2C\ell F_5$ (73%). The ratio of atoms, ^{12}C:^{19}F:$^{35}C\ell$, is 0.16:0.67:0.17 (in the event rate) and the average A is 20.7 so that the average target nucleus approximates ^{19}F.

About half of the neutrino events in this heavy liquid are accompanied by dark tracks at the interaction vertices. Our definition of dark tracks, for the scanning phase of the experiment, is that the bubble density is more than twice the minimum ionization and the momentum is less than 0.9GeV/c. They are mostly short stopping tracks referred to as stubs. Examples can be seen in Fig.2a,b. The observation of short dark tracks is affected by the optical resolution of the detector. The normal optics covers the range between $\ell_D>10$mm and $P_{proton}<0.9$ GeV/c with good efficiency. The holographic optics extends the sensitivity of our detector down to 0.5mm and covers the range, $0.5\text{mm}<\ell_D<10\text{mm}$. The multiplicity distribution of dark tracks, n_D, obtained by a careful examination of a sub-sample combining the data of both optical systems extends up to $n_D^{max}=9$ with an average multiplicity, $<n_D>=1.94$. (In data from the normal optics alone, $<n_D>=1.75$ with $n_D^{max}=7$.) Neutrino-deuterium interactions never contain this many stubs so that it is reasonable to assign them to nuclear debris. The extension of n_D up to nine indicates almost complete break up of the nucleus, even if it were $^{35}C\ell$.

The contamination of the primary dark track sample due to a combination of short $\pi^{\pm}$ decays and π^- interactions ($\pi^- \rightarrow$ neutrals) was less than 4%. These observed pions were removed from our dark track samples. It has been reported that 12% of dark tracks are deuterons in energetic hadron interactions[4]; however, we assume that all dark tracks are protons in the following analysis.

Fig.5 is the kinetic energy/momentum/length distribution of the dark tracks, where the data provided by normal optics and holography are normalized so as to agree in the region where they overlap. There is a peak below 20MeV followed by a continuum extending to higher energy. This feature is very similar to that observed from secondary proton emission in

energetic hadron-nucleus or photon-nucleus interactions.

Fig.6 shows a scatter plot of the momentum vs. the angle of emission of the dark tracks. The angular distribution is almost isotropic below $P_D = 0.35$GeV/c (T = 63MeV) and shows a broad forward enhancement above this value, where $P_D = 0.3$ GeV/c corresponds to $\ell_p = 3.7$cm for protons. The peak below 20MeV is the evaporation peak. The region above it is considered to be the pre-equilibrium region where the influence of the primary interaction is approximately preserved. Here, we presume that there is a difference in the production mechanisms of the short dark tracks (SDT) less than $\ell_p = 3.7$cm, $P_D = 0.35$GeV/c, and the longer dark tracks (LDT).

In the following, we will analyze dark track production on the basis of this classification. We separate the events into two groups by the absence or presence of dark tracks and also into sub-groups based on the length and multiplicity of dark tracks. These categories are the no dark track (ND), only short dark track (S), single long dark track (L1) and multiple dark track with at least one long dark track (L2).

Table I

	Event	$\langle n_h \rangle$	n_h^{max}
Total event	1132		
(ND) Events without dark track	570	4.99	12
(S) Only short dark tracks	242	5.21	12
(L1) Single long dark track	155	5.05	9
(L2) Multiple DT, at least one long DT	165	6.56	18

Analysis I

A sensitive way to discern the correlation between the dark track production and the primary neutrino-nucleon interaction is to examine the distribution of light hadron track multiplicity, n_h, which is a quantity directly associated with the primary neutrino-nucleon interactions. Fig.7 a,b,c,d are the n_h distributions for each group of Table I. The (ND) group shows the characteristic even-odd structure familiar in deuterium interactions. Because of the selection of quark flavour in neutrino interactions, the cross section of ν-n is about twice that of ν-p. It suggests that the events of this group are mainly produced by interactions with quasi-free nucleons. The (S) group also maintains the even-odd structure seen in the (ND) groups; however this feature is not present in the (L1) and (L2) groups. This shows that the nuclear disturbance in the primary neutrino-nucleon interactions increases in the order of (S), (L1) and (L2). The average value of n_h, $\langle n_h \rangle$, and n_h^{max} are also useful in deducing the amount of the disturbance. Table I shows that $\langle n_h \rangle$ and n_h^{max} increase from 4.99 and 12 for (ND) to 6.56 and 18 for (L2). The only possible cause for such increase in light hadron multiplicity is rescattering, the interaction of primary products in nuclear matter.

The momentum distribution of light hadrons, P_h, and their angular divergence, θ_h, are direct measures of the disturbance in the neutrino event. Fig.8 shows the net charge (NC) of light tracks (light hadrons plus muon) obtained from a clean subsample for (ND), (S), (L1) and (L2) groups. The net charge is originally 0 (ν-n events) or +1 (ν-p events). Events with a net charge of +2 or greater are due to the rescattering, and +3 or greater part indicates the existense of multiple rescattering. The considerable amount of -1 in the (L1) and (L2) group is due to the exclusion of a slow proton in the final state. The primary neutrino interaction can include a slow proton (direct proton) and the rescattering also can produce a slow proton. The net charge is a complicated

overlap of the effect of the increase of charge by rescattering and the decrease by slow proton loss, especially in the (L2) group. Therefore, we use the net charge data only for qualitative discussion, and in the correction to n_h to account for losses due to the slow protons.

Analysis II

An independent quantity which can be used to estimate the amount of invisible recoiling inside the nucleus is the following quantity, $E-Px$, where Px is the longitudinal momentum. For neutrino interactions on a nucleon,

$$E-Px=E_\nu-P_\nu$$
$$=(\Sigma E_{vis}+\Sigma E_{miss}-M_n)-(\Sigma P_{x,vis}+\Sigma P_{x,miss}+P_n)$$
$$=0,$$

where M_n is the target nucleon mass and P_n the Fermi momentum of the target nucleon. We define the observable quantity ε as the experimental E-Px value;

$$\varepsilon=(\Sigma E_{vis}-M_n)-\Sigma P_{x,vis},$$

If there are no missing particles and no Fermi motion, $\varepsilon=0$.

Any Fermi motion will result in the smearing of the quantity ε.

If there are missing particles, $\varepsilon=-(\Sigma E_{miss}-\Sigma P_{x,miss})<0$. Therefore, normally, $-M_n<\varepsilon<0$. When a charged particle from a primary neutrino interaction is not counted in ε for any reason, it appears as an increase of missing particles, and ε shifts toward negative values.

If a nucleon recoil occurs inside the nucleus and the recoil particle remains unseen or if the visible recoil proton is not counted in ε:

$$E-Px=(\Sigma E-M_n)+(E_{recoil}-M_n)-(\Sigma P_x+P_{recoil})$$
$$=0.$$

Thus, the shift, $\Delta\varepsilon$, of the observed ε caused by the recoil is:

$$\Delta\varepsilon=-(E_{recoil}-M_n)+P_{recoil}\approx P_{recoil}>0.$$

A positive value of ε or a positive shift of the ε distribution indicates an invisible momentum loss due to the nucleon recoil in the nuclear interior.

Fig.9 shows the ε distributions for the (ND), (S), (L1) and (L2) groups of this experiment and for ν-deuterium data[5]. In the case of ν-D, positive values of ε result only from the smearing caused by the Fermi momentum. (Fig.9a) The (ND) group has a typical distribution in the negative region and a small tail in the positive region. (Fig.9b) However, in the groups with dark tracks, (S) and (L2), the ε distributions have appreciable positive tails, (Fig.9b and d). The average value, $<\varepsilon>$, increases in the (S) and (L2) groups, which show the momentum loss due to recoil nucleons. An extrapolation of the relation between the fraction of the positive part and the difference of $<\varepsilon>$ in the different groups allows one to estimate the average momentum loss in the (ND) group due to the nucleon recoils to be 0.05GeV/c (1.4MeV) per event. This is a surprisingly small value.

The corrected momentum loss is 0.18GeV/c and 0.41GeV/c for the (S) and (L2) groups respectively, Table II.

Table II

	$\Delta<\varepsilon>$	Corrected
(ND)	0. GeV/c	0.05 GeV/c
(S)	0.128	0.18
(L1)	−0.007	0.04
(L2)	0.357	0.41

The (L1) group is special. Its ε distribution is quite similar to the (ND) group. These data show that the primary neutrino interactions in this group result in little nuclear disturbance. In spite of the existence of a dark track faster than 0.35GeV/c, the average momentum loss from ε is only 0.04GeV/c. This implies that the single long dark track of the (L1) group is mostly the direct proton.

Fig.10a,b show the n_h distribution for all events and the fraction of all dark track events, $F(n_h)$. This fraction is almost independent of n_h in the region of n_h where

most of the events occur. Since the rescattering will often yield slow protons, this independence proves that the formation of most of the final n_h particles occurred outside nucleus.

Fig.10c,d,e are the fractions of dark track events for the (S), (L1) and (L2) groups. It is flat in (S). In the (L1) group, Fig.5d, it shows a negative correlation, which is the result of the decrease of the value of n_h due to the exclusion of the direct protons. In the (L2) group, $F(n_h)$ shows a sharp rise above $n_h=13$, however, this sharp rise is only apparent and merely reflects the increase of n_h^{max}. In the (L2) group, the final multiplicity, n_h, was increased from that of (ND) group, by +1.6. This is a result of the combined effect of a track increase due to rescattering and a decrease due to slow direct proton. Fig.5f shows the $F(n_h-1)$ for the (L2) group, where the n_h distribution of (L2) was shifted one bin to left. It is seen that the n_h dependence is considerably moderated by this correction.

Summary of groups

The assignment of events to the (ND), (S), (L1) and (L2) groups is not perfect, since there is unavoidable mixing due to invisible backgrounds. However, it seems that each group is dominated by a characteristic feature.

(a) No dark track group (ND): Events without visible short stubs or dark tracks. The even-odd structure of the n_h distribution shows that the rescattering of secondary particles is very small. The small fraction of events with a net charge above +1 is explained by a small amount of invisible nucleon recoil. One would expect this group to include events with only invisible neutron recoils. However, the high multiplicity of dark track, $<n_D>_{vis}=1.94$, provides an explanation. Assuming that the production rate of slow neutrons is the same as that of visible dark tracks, we find that the number of events with only neutron recoils is $(1/2)^{1.94\times2}=7\%$ of dark track events, equivalent to only 10% of the (ND) events. The average momentum loss due to nucleon recoils is 0.05GeV/c (1.4MeV) per event, which indicates that the presence of the nucleus has very little effect on the neutrino interactions for this group of events. Therefore, the (ND) events can be used as a reasonable sample of neutrino interactions with quasi-free nucleons. This provides the justification for the assumption used to discuss the EMC effect in reference 1. We will also use this group (ND), instead of deuterium data, to represent a control sample of events with minimal rescattering.

(b) Short dark track group (S) : Events with only short stubs below 0.35GeV/c. The multiplicity of short stubs extends to 4 with an average value of 1.42, and the angular distribution of the stubs is almost isotropic (Note Fig.6 contains only the normal picture data). This is typical of an evaporation phenomenon. The even-odd structure of the distribution is similar to that of the (ND) group. Therefore, the production of short stubs is almost independent of the neutrino interactions. The mechanism may be similar to the production of spectator protons in neutrino-deuterium interaction. We conclude that this group reflects only pure binding energy effects relating to the interacting nucleon.

(c) (L1) group : Events with only a single long dark track, faster than 0.35GeV/c, have a special feature. The E-Px analysis shows that the momentum loss to the nucleus is only 0.04GeV/c per event despite the existence of a dark track faster than 0.35GeV/c. The net charge of -1 and the negative correction of the $F(n_h)$ distribution both indicate that the direct proton was counted as a dark track. A Lund simulation for this experiment shows that the rate for such slow direct proton production is about 10% and the fraction of slow protons below 0.35GeV/c is less than 0.7% of all events.

(d) (L2) group : Events with multiple dark tracks but at least one long dark track (>0.35GeV/c). The multiplicity of long dark tracks extends to 6. In this group, the even-odd structure in the n_h distribution is completely destroyed, $\Delta<n_h> = 1.8$ and n_h^{max} extends to 18. These data show that the rescattering of secondary particles is a prominent feature of this group. This group includes both LDT and SDT. The correlation between the production of LDT and SDT is weak. (SDT = 0.2 + 0.2·LDT) per event. Fig.11c, d are the angular distributions of short and long dark tracks respectively in the (L2) events. It shows the evaporative feature of the SDT. Therefore, some portion of SDT is due to evaporation which is independent of LDT production and some portion is due to evaporataion associated with the LDT production. The considerable number of events which have a net charge of −1 indicates that some of the LDT can be the direct protons as shown in the (L1) group.

Our picture for the dark track production based on the above data is as follows. The nucleon which interacted with the neutrino was correlated with surrounding nucleons. When this nucleon suddenly moves, a recoil momentum is given to the surrounding nucleons. If the correlation between the interacting nucleon and the neighboring nucleons is negligible, we have (ND) events. ($P_{recoil} \approx 0.05$GeV/c per event) If the correlation is non-negligible, the recoil momentum is given to the nucleus and resulting evaporation, (S) group. ($P_{recoil} \approx 0.18$GeV/c per event) Another kind of correlation between the nucleus and the neutrino interaction occurs in the rescattering. After the fragmentation and formation of particles from the neutrino-necleon interactions, these primary particles can interact with nucleons inside nucleus (inelastic and elastic) and eject them as recoil nucleons. These recoil nucleons have a directional correlation with the incident neutrino. This ejection can further be followed by the evaporation of nucleons as same as in the (S) group. Some of the long dark tracks in the (L1) and (L2) groups are the direct protons.

EMC EFFECT

We have shown above that the (ND) group is a reasonable sample of events which occurred on quasi-free nucleons, with the remaining groups typifying interactions with more tightly bound nucleons. If this is correct, we should see the EMC effect in the ratio of the x distribution of other group relative to the (ND) group. Fig.12a shows this ratio of x distribution for the all dark track group (S + L1 + L2), which shows an EMC effect corresponding to ref.1.

However, for the (L1) group, we have pointed out that the LDT is a direct slow proton from the primary products of the neutrino interaction. The probability of including a slow proton in the primary products is high for small x events. Therefore, for this group, the ratio drops as x increases, but will not rise at large x [6], Fig.12c. This is merely a reflection of the kinematical selection of this group. The (L2) group also includes some direct proton events as well as some hadron rescattering. The interpretation for this group is not straight forward, Fig.12d.

However, the dark stubs in the (S) group are the nuclear debris arising from the thermalization of the excited nucleons or from the pre-equilibrium condition which resulted from the strong correlation between the struck nucleon and its surrounding nucleons (the nuclear binding effect). Therefore, we conclude that the ratio of the (S) group, Fig.12b, is clearest choice to reflect purely nuclear effects (EMC effect).

FORMATION-RESCATTERING

Fraction of rescattered events

The smearing of the n_h distribution, the increases of $\langle n_h \rangle$ and n_h^{max}, and the events for which the net charge exceeds +1 all indicate the existence of rescattering. We use the increase of n_h in each group relative to the (ND) group, $\Delta\langle n_h \rangle$, as the measure of the rescattering in each group, Table III.

Table III

	Corrected $\langle n_h \rangle$	$\Delta\langle n_h \rangle$	f_{rs}	f_{ev}
(ND)	4.99	0.10	0.06	0.05
(S)	5.31	0.42	0.25	0.19
(L1)	5.43	0.54	0.32	0.24
(L2)	7.12	2.23	1.33	1.00
Total			0.32	0.24

The correction to n_h is for the slow protons missing from the final hadron multiplicity, n_h. The correction on $\Delta\langle n_h \rangle$ includes a bias of 0.10 to account for the rescattering present in (ND). The rescattering probability is given by

$$f_{rs} = \Delta\langle n_h \rangle / M,$$

where M is the average multiplicity increase per rescattering which is given by

$$M = \frac{\int \left[n_h(P_h) - \frac{2}{3} \right] \sigma(P_h) \cdot (dn/dP_h) dP_h}{\int \sigma(P_h) \cdot (dn/dP_h) dP_h} .$$

Assuming that all light track hadrons are pions for simplicity, and using the hadron multiplicity[7], $n_h(P_h)$, and the inelastic cross sections in $\pi^{\pm}p$ interactions[8], we obtain M=1.7, when the upper limit of integration is 8 GeV/c. The correction 2/3 is based on the hypothesis that the rescattering is caused by neutrals half as often as by charged particles.

The f_{rs} in Table III is the rate of rescattering per event and f_{ev} is the fraction of events for which there is one or more rescatterings. The rescattering is mostly concentrated in the (L2) group. It seems that virtually all events of this group include rescattering. In the following, we will use the (L2) group as a sample of rescattered events. Other groups contain a significantly smaller amount of rescattered events. The average rescattering probability in event number is $f_{ev}=0.24$ per event while the average number of rescatters per event is $f_{rs}=0.32$. This yields a ratio of multiple rescattering to single rescattering of ~0.4. A systematic uncertainty of ~20% due to our estimate of M is expected in f_{rs}; however, this will not affect our conclusions meaningfully.

Quark interaction

One could imagine that a possible source of the rescattering, independent of n_h, is the rescattering caused by the rapidly moving part of the excited nucleon or the energetic struck quark. The struck quark moves through the nucleus with an energy of ~ν in the direction of the neutrino. In general, we can expect an elastic type interaction whose rate is 13% and 9% at 10 and 50 GeV/c, respectively, in πp interactions[8]. However, no recoil peak is observed around 90° in any angular distribution of dark tracks, Fig.11. This negates the possibility that the observed rescattering is due to elastic type scattering by the energetic part of excited nucleon or struck quark system.

Rescattered events

We now study the rescattered events using the (L2) group as a prototype sample of rescattered events while the (ND) group will be used as a control sample having minimal rescatterings. Fig.13 shows the comparison of the hadronic momentum (P_h) distributions in the (L2) and (ND) groups for three regions of ν, where the distributions are normalized to numbers of particles per event. With this normalization

the difference between the two histograms directly shows the actual increase (hatched area) or decrease of tracks caused by the rescattering. Since systematic bias in the differences is negligible, only the statistical error remains here. An enhancement of the soft component, the secondary products of rescattering, is prominent below 1GeV/c in all regions of ν and seems to extend up to the average value $<P_h>$, reaching 5GeV/c. In an adjacent region, the attenuation of source particles and the enhancement of secondary products could overlap. The hadrons above 5GeV/c must be included in the source of rescattering.

Fig.14 shows the comparison of the normalized z distributions for the same two groups in each region of ν. The soft component produced by the rescattering is concentrated at values of z below 0.05 with minor values extending to higher z.

Fig.15 shows the similar comparisons of both groups as a function of rapidity in the CM system of hadrons. It shows clearly that the enhancement of the soft component is in the backward and central regions ($y_{CM}<1.$). The central region moves with γ_W. The attenuation due to rescattering is seen in the forward direction. The attenuation in the backward region is obscured by the above backward enhancement of the soft component. The fraction of the hatched area decreases for the higher ν region, because the ratio $\Delta<n_h>/<n_h>$ decreases with ν. Table IV summarizes the CM rapidity distributions. The entries in the table refer to $<n_h>^t$, the average numbers of light hadron tracks per event in the forward (F) and backward (B) hemispheres. In the (ND) group, the track multiplicity is larger in the forward than in the backward direction. This situation is reversed in the (L2) group because of the rescattering. The attenuation in the forward direction, $<n_h>^t_{L2} < <n_h>^t_{ND}$, is clearly present.

Table V $<n_h>^t$

ν GeV	(ND)		(L2)	
	F	B	F	B
0-30	1.90	1.46	1.65	2.47
30-60	2.87	2.44	2.84	3.67
60-100	3.39	2.70	3.13	3.57

Dependence on event variables

Fig.16a,b,c,d show the $<n_h>$ distributions of the all dark track events (S+L1+L2) and (ND) events and their difference, $\Delta<n_h>$, as a function of W, ν, γ_W and Q^2. Essentially, they represent the presentation of our data from four slightly different perspectives. (Fig.3) The flat distributions of $\Delta<n_h>$ suggest the independence of rescattering on any event variables. In order to estimate the value of resacttering probabil;ity, we use the average increase of $<n_h>$ in all events, $\Delta<n_h>_{all}$,

$$\Delta<n_h>_{all}=\left(<n_h>_D-<n_h>_{ND}\right)\cdot\left(\frac{D\ event}{D\ event+ND\ event}\right)$$

By dividing this quantity by the multiplicity increase per rescattering, we obtain the rescattering probability $f_{rs}=\Delta<n_h>_{all}/M$. Fig.16e,f,g,h show the f_{rs} for each region of the event variables. We conclude that the rescattering probability is independent of these variables at our level of statistics.

The plots for W, ν and γ_W are equivalently the plots for $<n_h>$. The $<n_h>$ varies from 2.7 to 6.5 with W as seen in Fig.16a. Therefore, the above independence is equivalent to the independence of the rescattering probability on $<n_h>$.

Formation length

The data in Table III show that some hadrons were formed inside the nucleus and subsequently rescattered. About 24% of the

events exhibit rescattering, and the number of rescattering is 0.32 per event.

These data negate the primitive concept that all hadrons were formed at the point of the neutrino interaction. If this were the case, we would expect a rescattering rate which is totally at variance with our data. Thus:

$f_{rs} = 5.0(1-\exp(-2.4/\ell_m)) = 2.1$ per event,

where 5.0 is the mean multiplicity of the (ND) event and 2.4fm is the average interaction distance from the neutrino interaction to the back surface of nucleus, (2/3R in fm). ℓ_m is the mean free path of hadrons inside the nucleus, $\ell_m = (\sigma A/(4/3)\pi R^3)^{-1}$, for which we assume a value of 4.4fm for pions, corresponding to $\sigma_{inel}(\pi N) = 21$mb. Therefore, we must introduce an artifact which suppresses the formation of hadrons inside the nucleus. Here, we assume a uniform spherical nucleus, $R = 1.3A^{1/3}$ [9].

We have shown that the rescattering is almost independent of n_h. This requires that the number of mesons formed inside the nucleus be approximately constant. The number of mesons formed inside the nucleus per event, N_f, is not known. We begin with the trivial observation, $0.8 < N_f < \langle n_h \rangle$. The lower bound is due to the observed $f_{rs} = 0.32$ in conjunction with the average interaction distance 2.4fm, $0.8 = 0.32/(1-\exp(-2.4/4.4))$. For the upper bound, if the number of formed mesons is too large, say 4, we should see an apparent n_h dependence in the region, $n_h = 1-6$ in Fig.5, which is contrary to our data. In order to have a considerable amount of multiple rescattering, multiple/single ≈ 0.4, the binomial distribution requires the average N_f should be the order of 2.

In order to suppress the formation-rescattering rate to fit the data, we involve the idea of a minimum formation length for hadrons[10,2]. The geometrical picture is as shown in Fig.17. The first hadron is formed at ℓ_f^{min} from the interaction point, and the second one follows with some delay etc. Assuming the step function probability for the formation as shown in Fig.17, and defining a as the formation probability after ℓ_f^{min} per length per event, the observed rescattering probability satisfies,

$$f_{ev} = \int (dV/V_0)\, a\, (\text{form} - \text{rescatt prob in t}),$$

where $V_0 = 4/3\pi R^3$.

The volume fraction, $VF(\ell_f^{min}) = \int dV/V_0$, provides the main suppression factor. The average travel path after the formation is $\ell_{rs} = \langle t \rangle$, and the average number of formed hadrons is $N_f = a \cdot \ell_{rs}$. For $N_f \approx 2$, we obtain the, formation length $\ell_f^{min} \approx 2.4$fm, volume fraction VF ≈ 0.54, and the travel path $\langle \ell_{rs} \rangle \approx 1.6$fm for the observed rescattering. The diameter of the nucleus is 7.1fm. Since the spatial extent of the nuclear surface is included in the travel path, the nuclear surface can only marginally affect the value of ℓ_f^{min}. The formation length was defined as the distance required to form a particle which has an interaction cross section of $\sigma \approx 21$mb on nucleons.

In summary, in approximately half of the events, ~2 pions are formed inside the nucleus with $\ell_f^{min} \approx 2.4$fm which cause the observed rescattering in a path length of $\ell_{rs} \approx 1.6$fm. On average, approximately 1 particle out of the 5 final hadrons per event were formed with $\ell_f^{min} \approx 2$~3fm inside the nucleus and a third of these provided the observed rescattering. The remaining 4 hadrons per event were formed outside nucleus. This is the first direct data relating to the concept of a formation zone[10].

SUMMARY

Dark tracks produced in the neutrino-nucleus interactions were studied. Events were classified by using the dark tracks. The no dark track events were used as a sample of events which occurred on quasi-free nucleons with minimal rescattering. The ratio of the X distribution of each group to the (ND) group

shows the EMC effect. However, the ratio of the (S) group is considered to reflect a purely nuclear effect.

Rescattering occurs in 24% of the ν-$A^{20.7}$nucleus interactions. They are mostly concentrated in the (L2) group. The rescattering was investigated by using the (ND) group as a control sample. The rescattering probability does not show a noticeable n_h dependence. The struck quark is not the source of the observed rescattering. Multiple rescattering is comparable with the single rescattering. It requires the formation of ~2 particles in about a half of the events. This results in an minimum formation length of $\ell_f^{min}=2\sim3$fm for the observed rescattering. The soft component produced by the rescattering preferentially populates the backward hemisphere. The source of rescattering may be mainly in the central/backward region but it spans the full center of mass solid angle. The momentum of source meson can extend to 10GeV/c in LS.

The formation and rescattering probability is independent of such event variables as W, ν, γ_W, Q^2, and n_h within errors.

Acknowledgement

This Research is supported by the US-Japan Cooperation Program on High Energy Physics between the Ministry of Education, Science and Culture, Japan, and the Department of Energy, U.S.A.. Also, this work is partly supported by the National Science Foundation of U.S.A.. We thank them for their support.

References

1. T.Kitagaki et al., Phys.Lett. B 214, 281 (1988)
2. W.Busza et al., Phys.Rev.Lett. 34, 836 (1975)
   D.Chaney et al., Phys.Rev.Lett. 40, 71 (1975)
   L.S.Osborne et al., Phys.Rev.Lett. 40, 1624 (1978)
   C.De Marzo et al., Phys.Rev. D 26, 1019 (1982)
   A.Bialas et al., Phys.Lett. 133B, 241 (1983)
   A.Arvidson et al., Nuclear Physics B246, 381 (1984)
   P.B.Renton, 3rd conf. on the Intersections between Particle and Nuclear Physics, Rockport, May (1988)
3. J.Hanlon et al., Phys. Rev. Lett. 45, 1817 (1980)
4. J.L.Bailly et al., Zeit. f.Phys. C 35, 301 ((1987)
5. T.Kitagaki et al., Phys.Rev. D28 431 (1988)
6. C.Ishii et al., Phys.Lett. B 216, 409 (1989)
7. J.Whitmore et al., Phys.Rep. 27C, 197 (1976)
8. Berkeley, CERN, Particle Properties Data Book (1988)
9. H.R.Collard et al., Landolt-Börnstein, New series, Vol.2, Nuclear Radii (1967)
10. L.D.Landau and I.Ya.Pomeranchuk, Doklady Akademii Nauk SSSR, 92 535(1953), ibid., 92, 735(1953)

Fig. 1 Tohoku 1.4m High Resolution Bubble Chamber

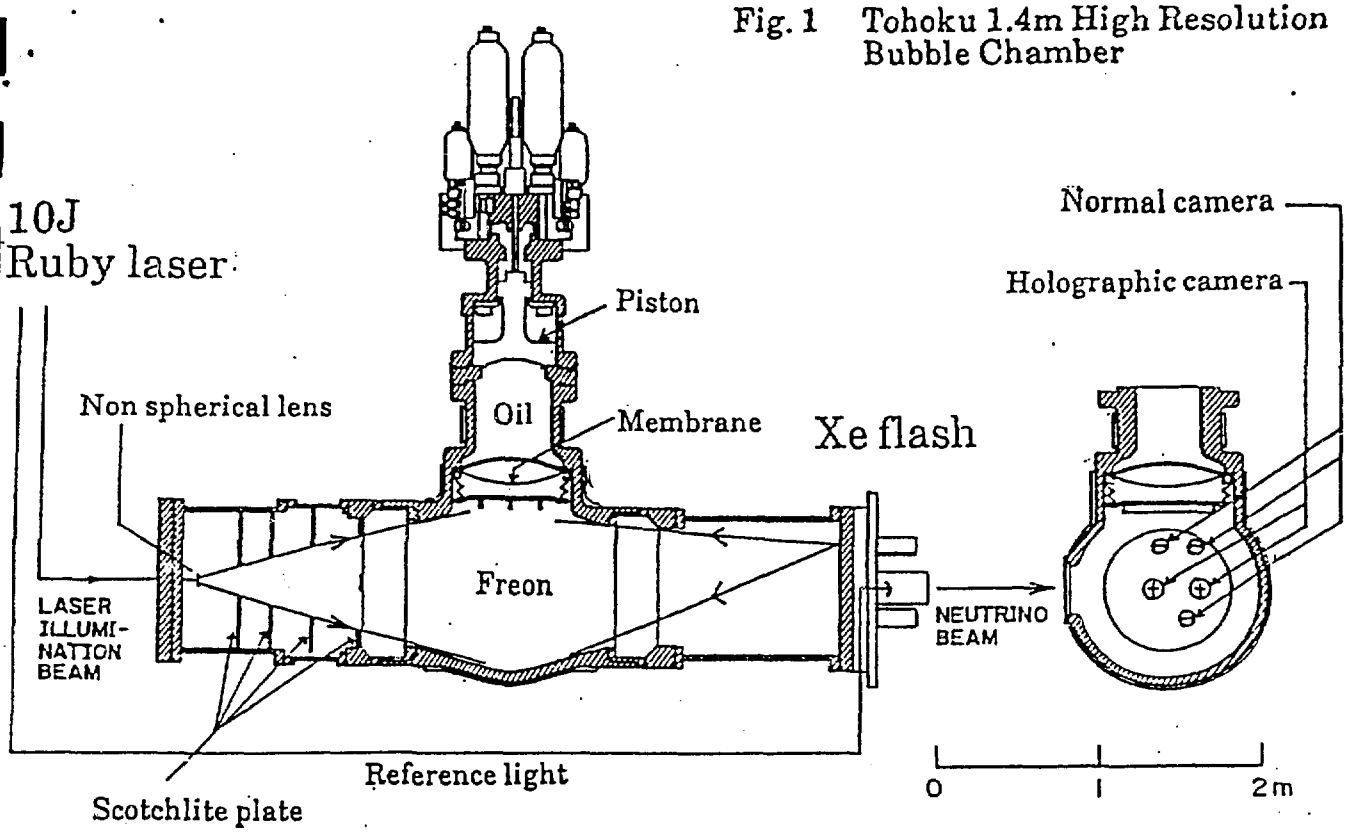

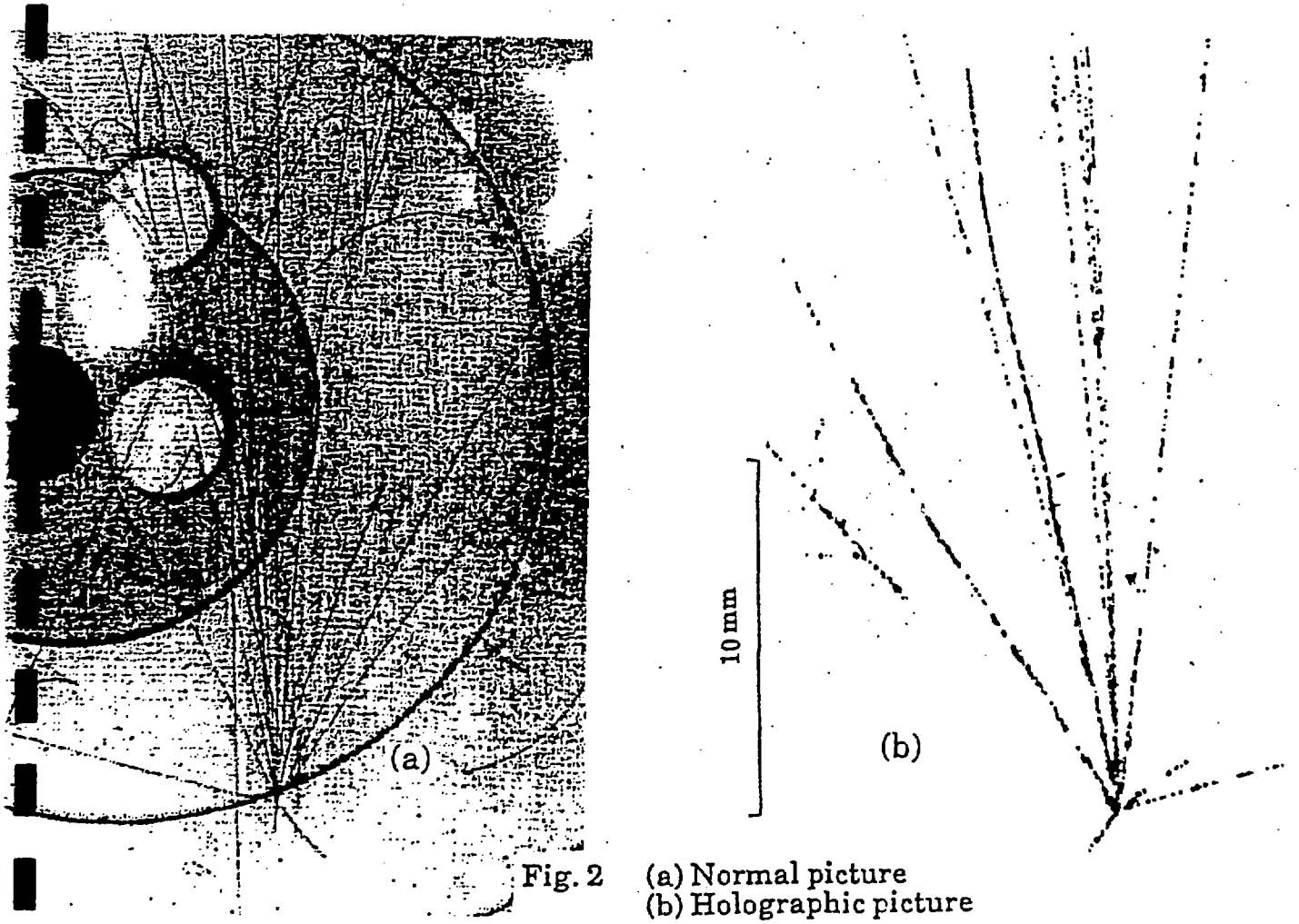

Fig. 2 (a) Normal picture
(b) Holographic picture

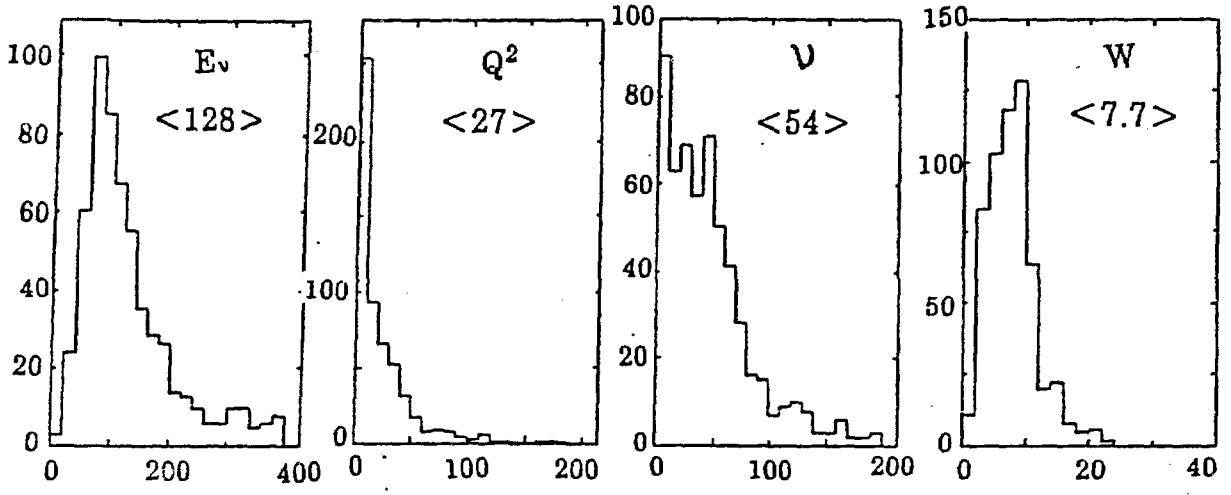

Fig. 3 E745 : Eν, Q^2, ν, W, γ_w

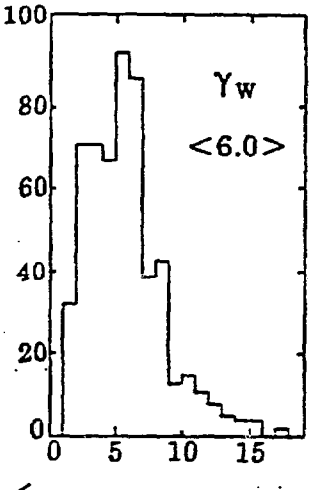

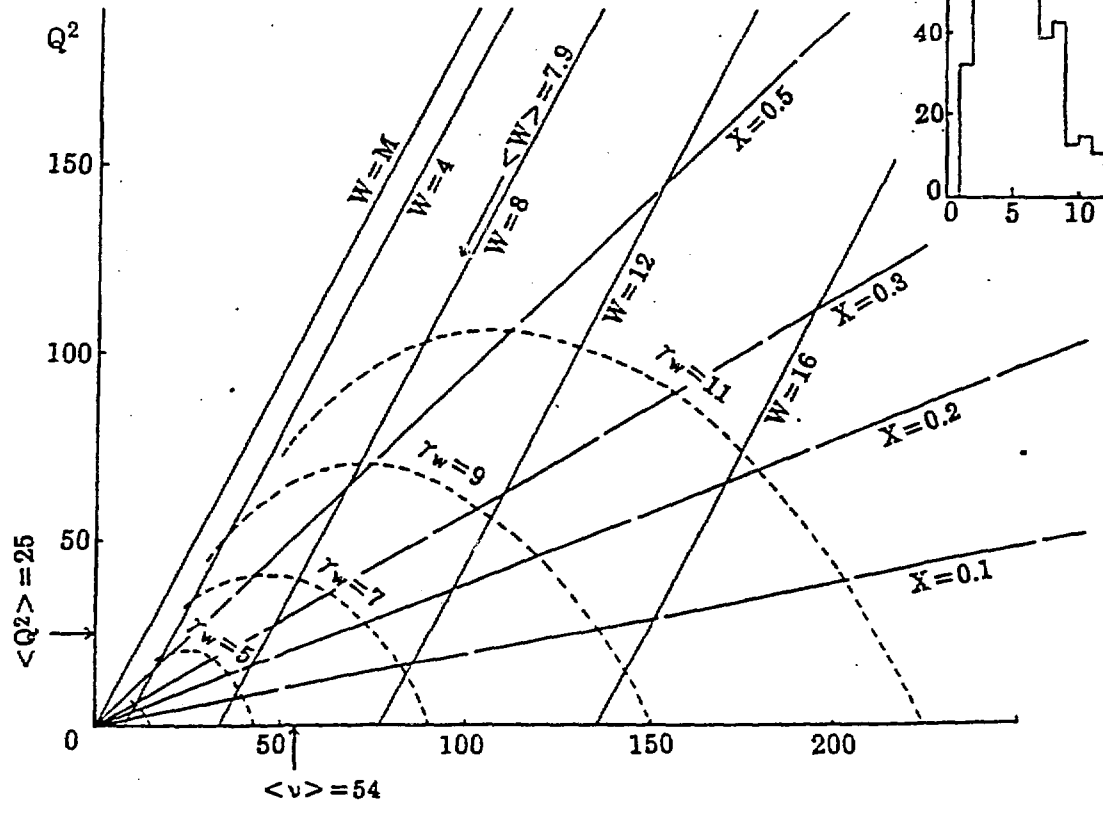

Fig. 4 Kinematics

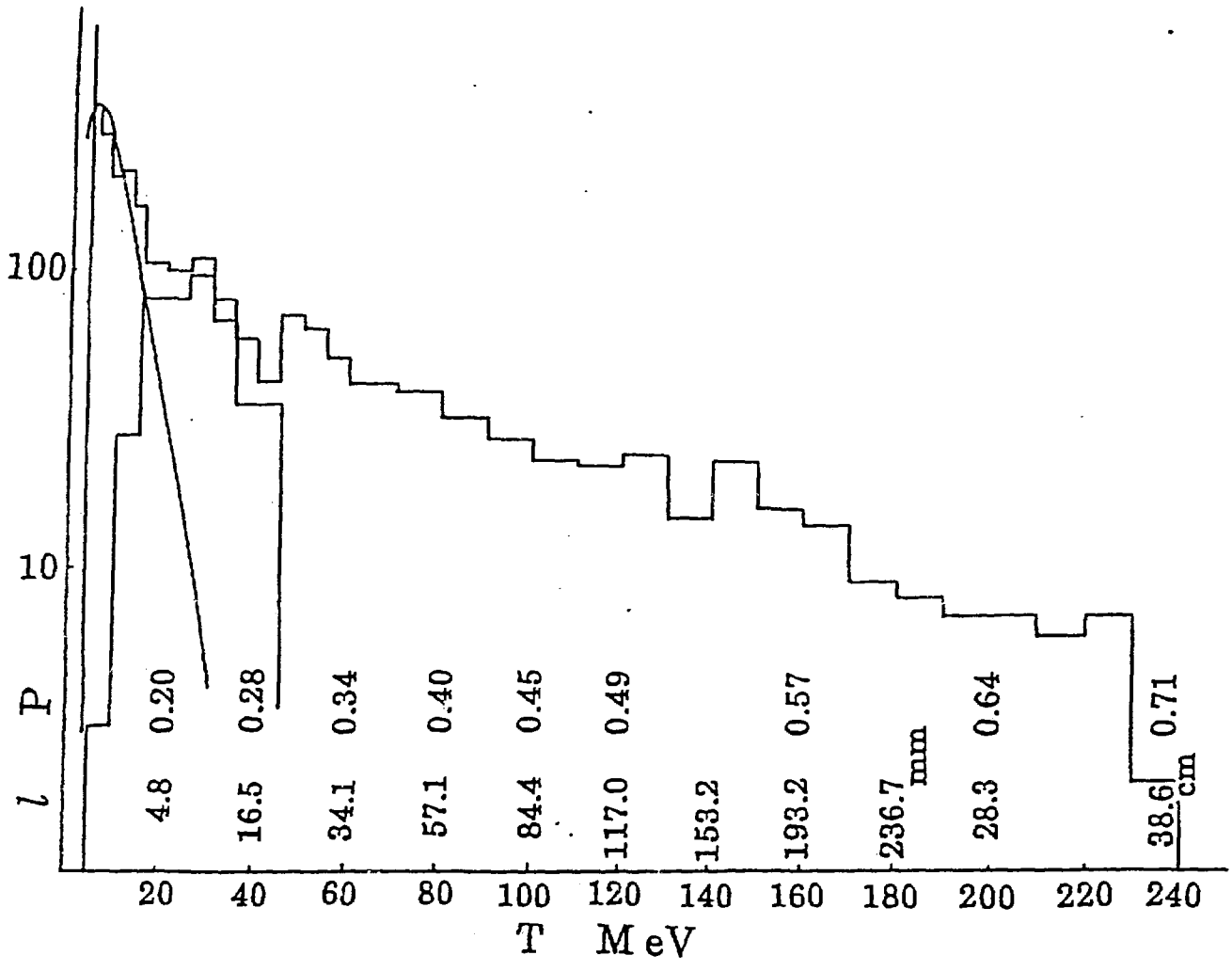

Fig.5 Kinetic energy/momentum/length distribution of dark tracks. Normal picture data (right) and holographic data are connected at 30MeV.

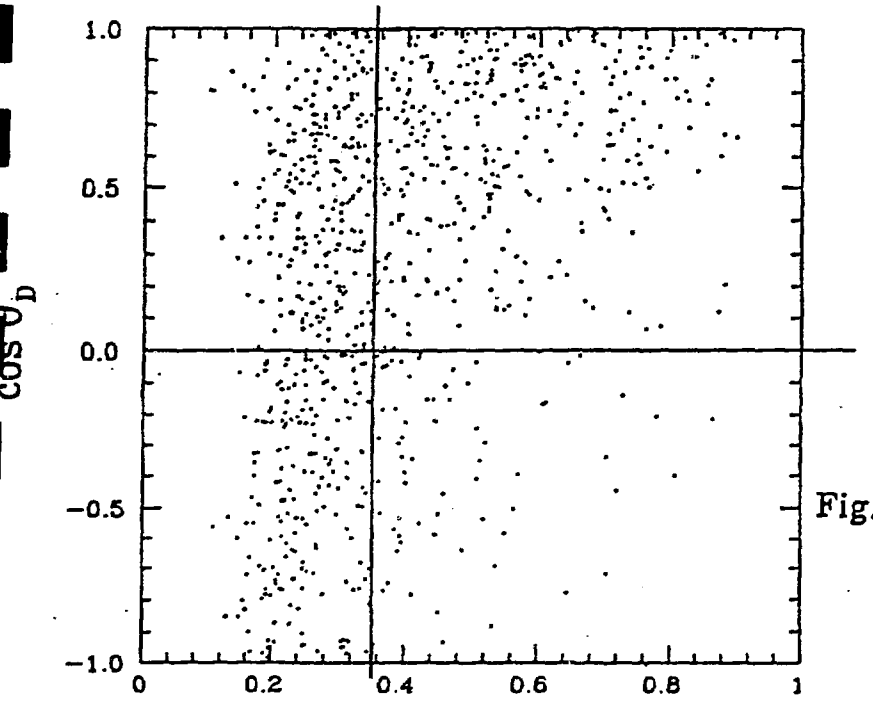

Fig. 6 Dark tracks, momentum, P_D, and angular distribution, $\cos\theta_D$.

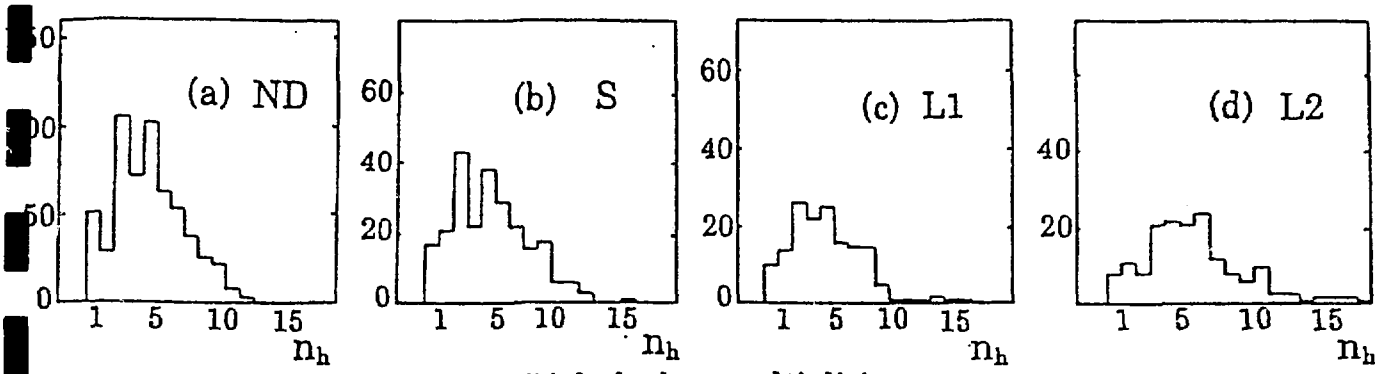

Fig.7 Light hadron multiplicity, n_h

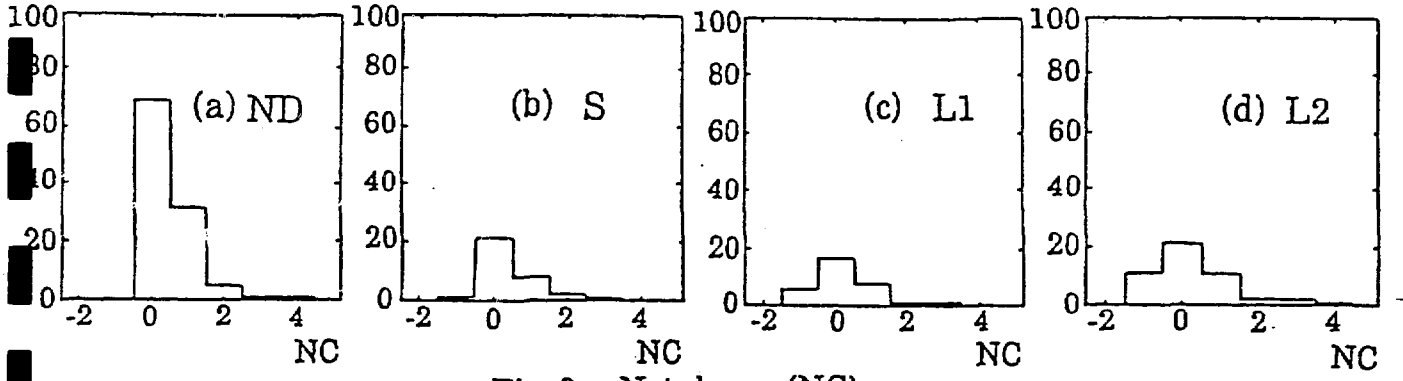

Fig. 8 Net charge (NC)

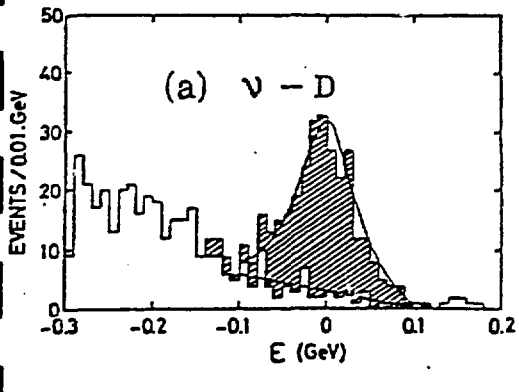

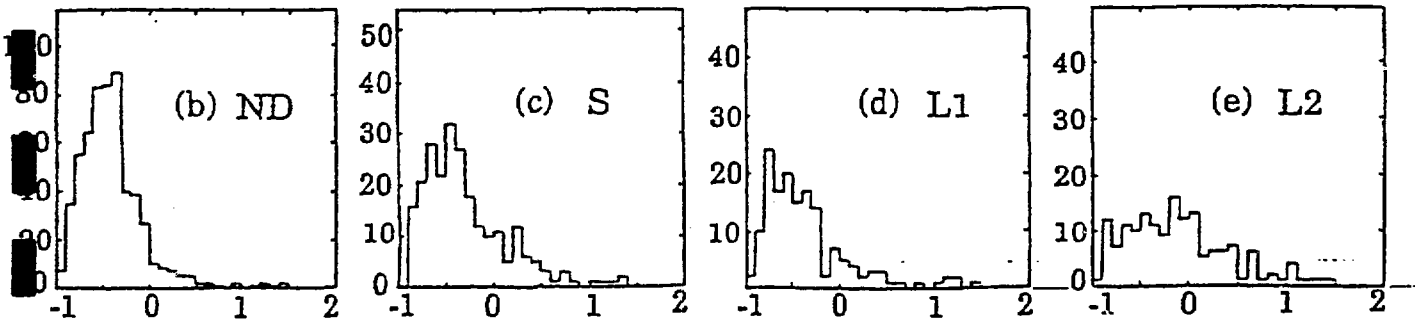

Fig.9 ε distribution, see text,

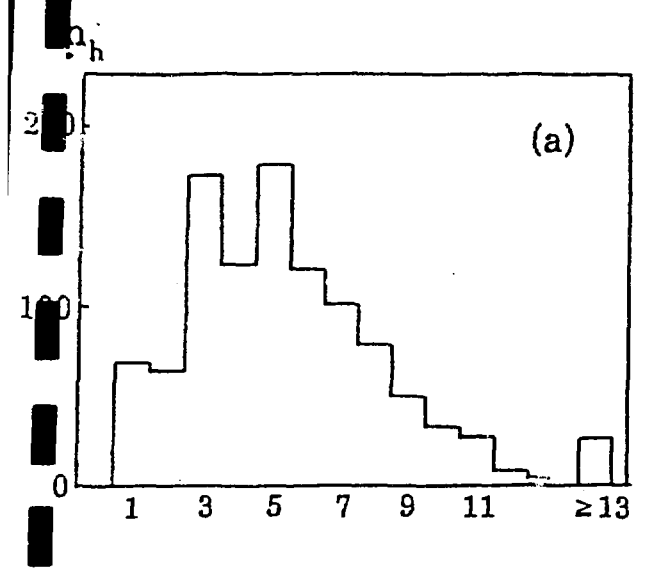

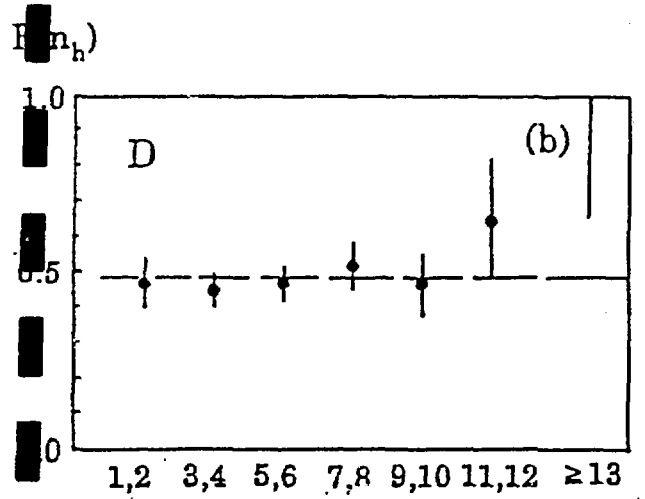

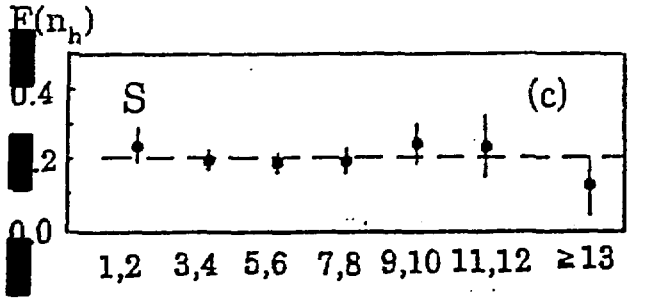

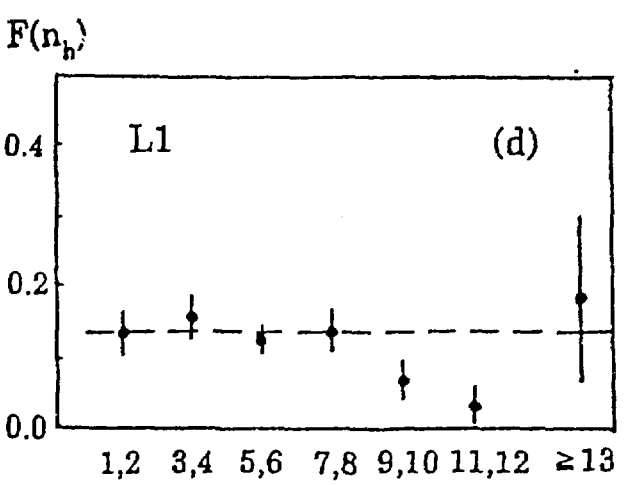

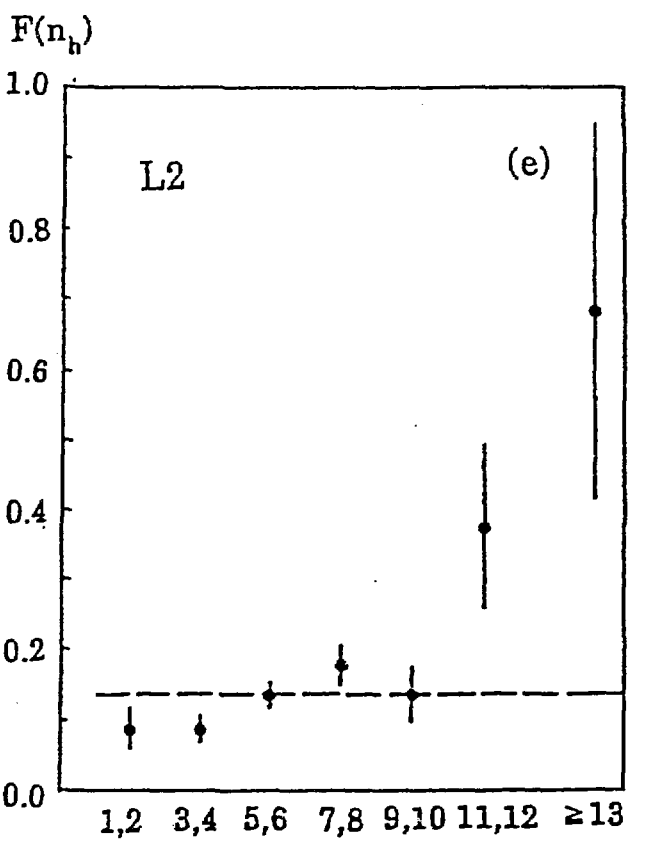

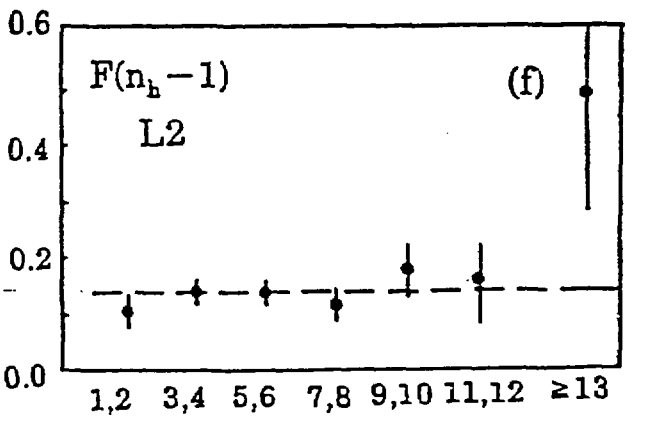

Fig. 10 Fraction of dark track events, $F(n_h)$

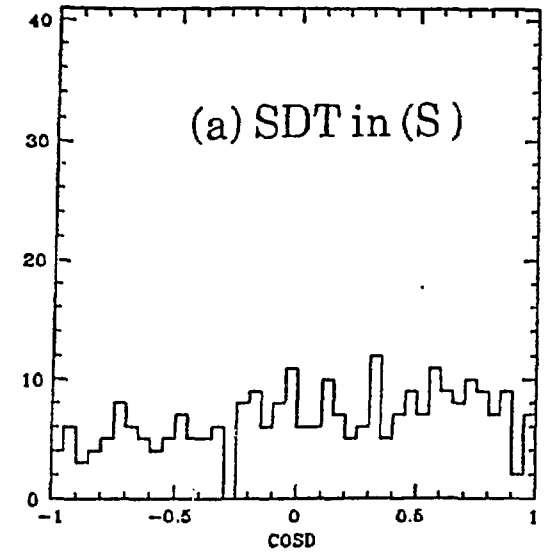

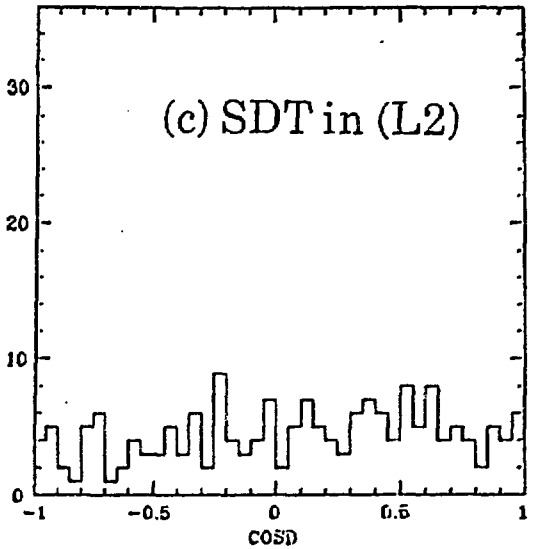

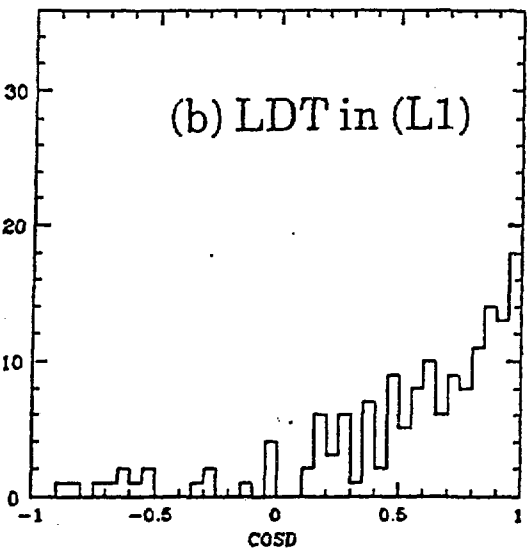

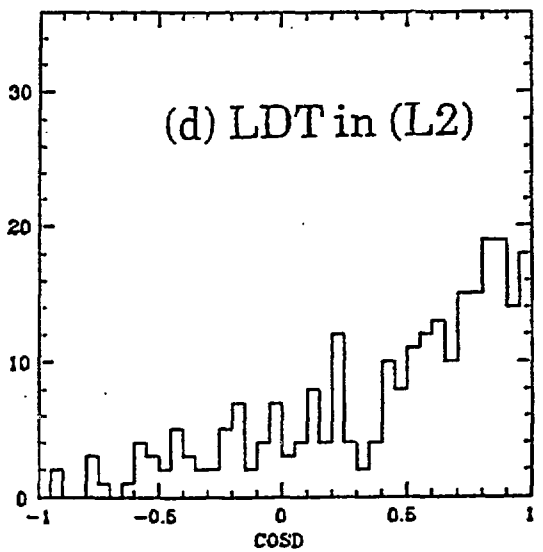

Fig. 11 Angular distribution of dark tracks

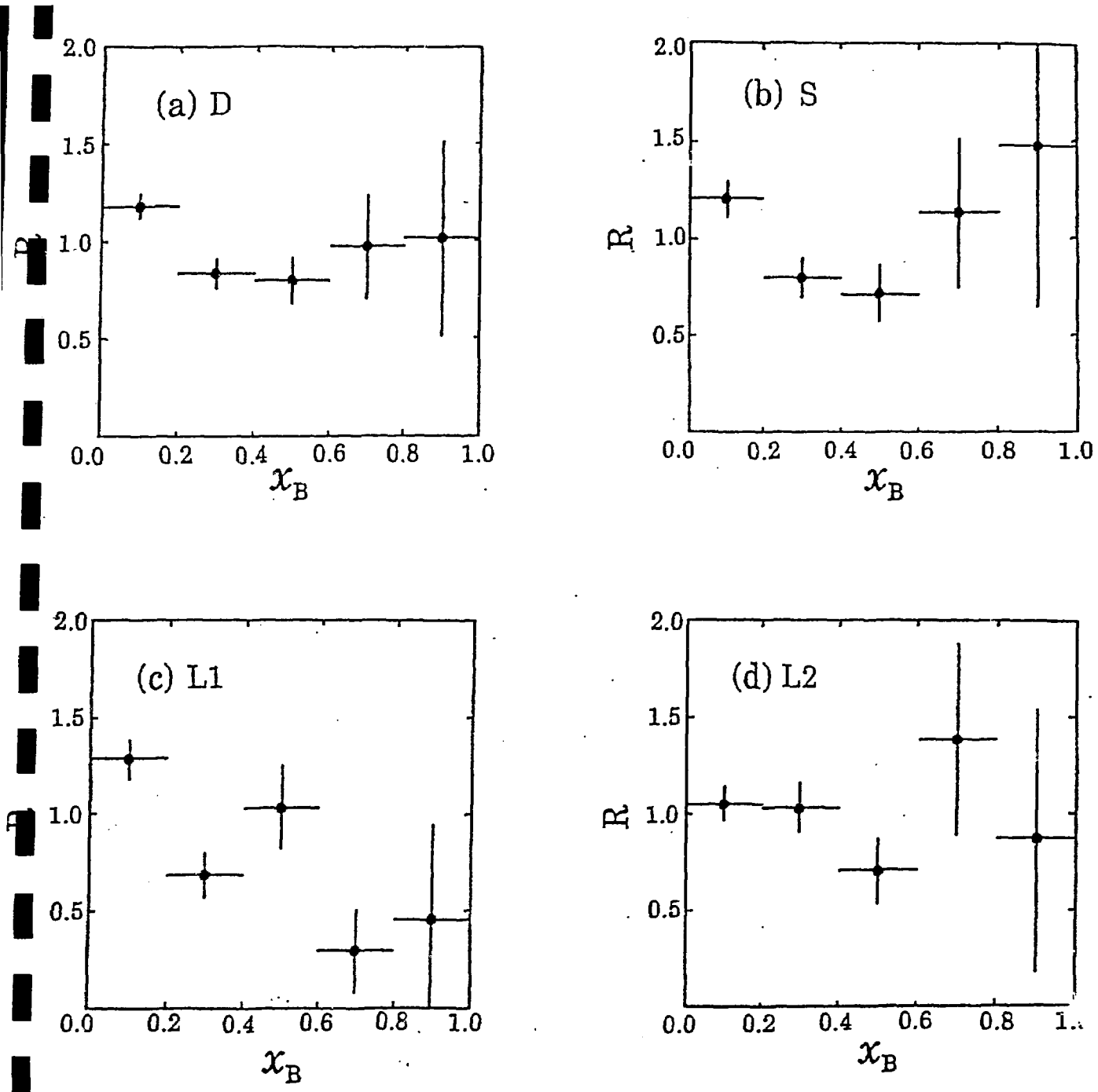

Fig. 12 EMC effect

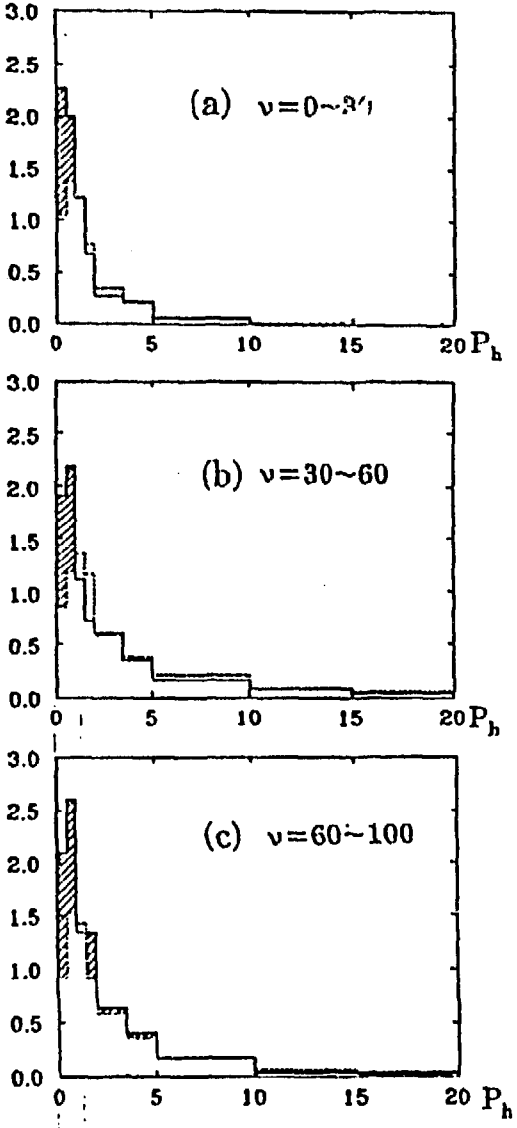

Fig.13 P_h distributions in ν regions
——— (L2) group
····· (ND) group

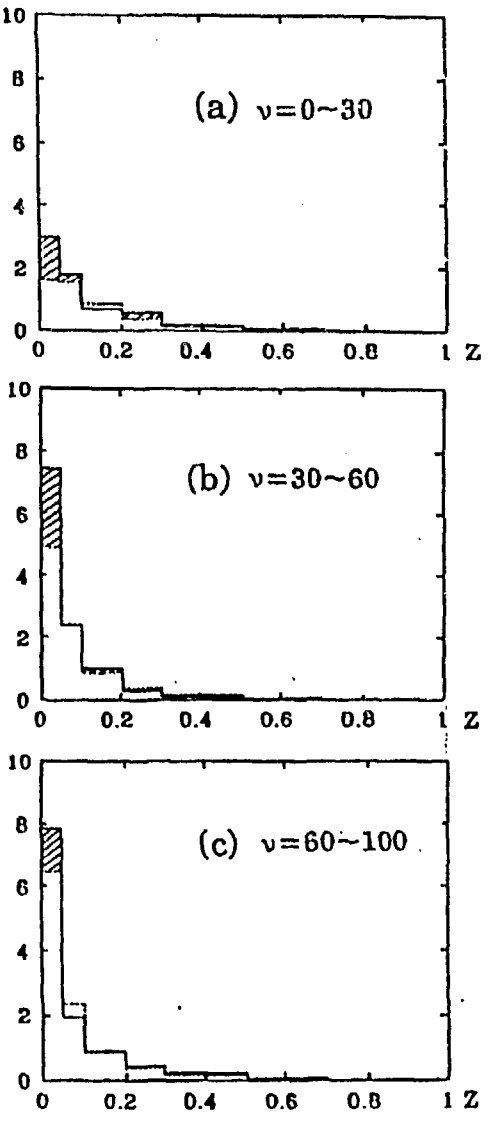

Fig. 14 Z distributions in ν regions

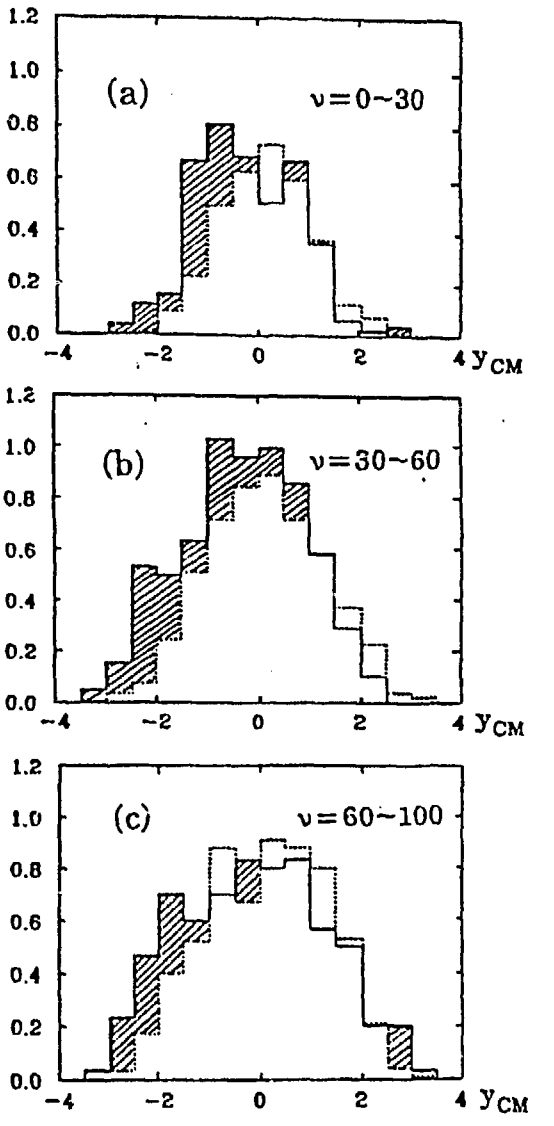

Fig. 15 y_{CM} distributions in ν regions

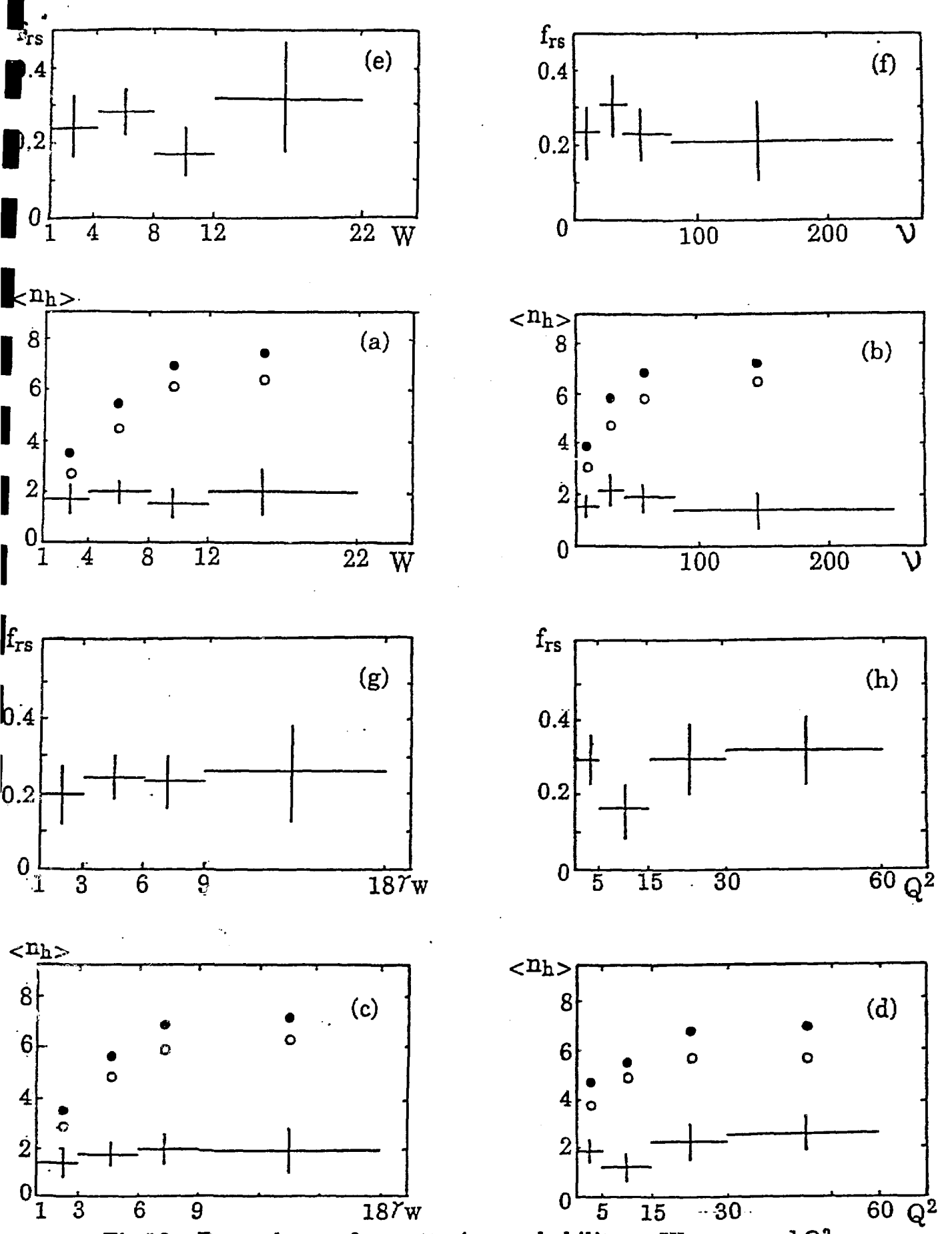

Fig.16 Dependence of rescattering probability on W, ν, γ_w and Q^2.
(a b c d) $\langle n_h \rangle$ in (D) and (ND), and the difference $\Delta\langle n_h \rangle$.
(e f g h) Rescattering probability f_{rs}

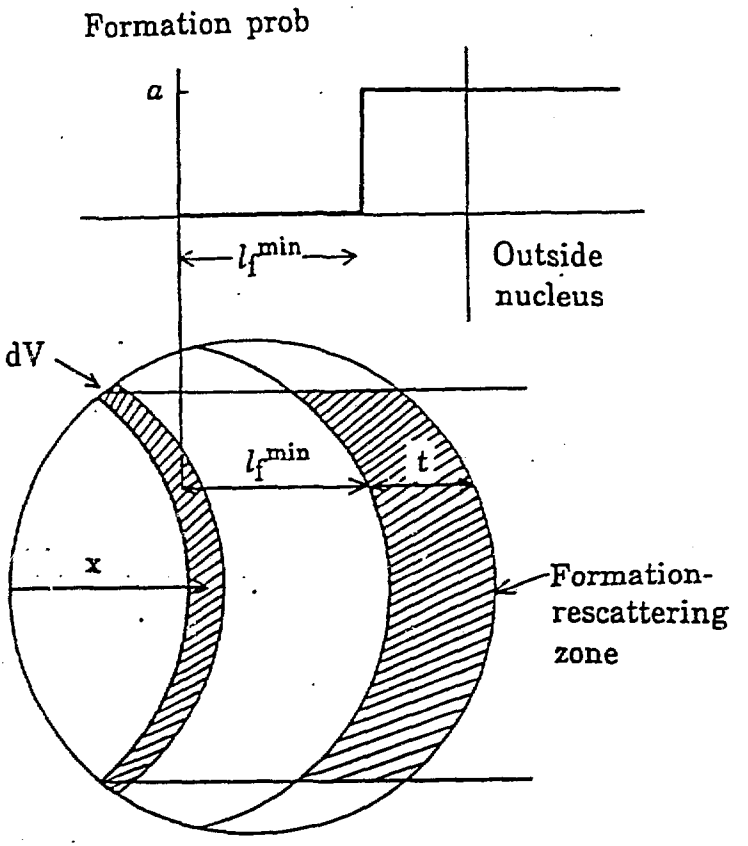

Fig.17 Minimum formation length, l_f^{min}